



Cite this article: Prakash A, Monteiro A. 2018 *apterous A* specifies dorsal wing patterns and sexual traits in butterflies. *Proc. R. Soc. B* **285**: 20172685.
<http://dx.doi.org/10.1098/rspb.2017.2685>

Received: 1 December 2017

Accepted: 29 January 2018

Subject Category:

Development and physiology

Subject Areas:

developmental biology, evolution,
molecular biology

Keywords:

apterous, dorsal–ventral differentiation,
butterfly wing patterns, developmental
constraints, eyespot repression

Authors for correspondence:

Anupama Prakash
e-mail: anupama@u.nus.edu
Antónia Monteiro
e-mail: antonia.monteiro@nus.edu.sg

Electronic supplementary material is available
online at [https://dx.doi.org/10.6084/m9.
figshare.c.3998226](https://dx.doi.org/10.6084/m9.figshare.c.3998226).

apterous A specifies dorsal wing patterns and sexual traits in butterflies

Anupama Prakash¹ and Antónia Monteiro^{1,2}

¹Department of Biological Sciences, National University of Singapore, Singapore, Republic of Singapore

²Yale-NUS College, Singapore

AP, 0000-0001-6922-2806; AM, 0000-0001-9696-459X

Butterflies have evolved different colour patterns on their dorsal and ventral wing surfaces to serve different signalling functions, yet the developmental mechanisms controlling surface-specific patterning are still unknown. Here, we mutate both copies of the transcription factor *apterous* in *Bicyclus anynana* butterflies using CRISPR/Cas9 and show that *apterous A*, expressed dorsally, functions both as a repressor and modifier of ventral wing colour patterns, as well as a promoter of dorsal sexual ornaments in males. We propose that the surface-specific diversification of wing patterns in butterflies proceeded via the co-option of *apterous A* or its downstream effectors into various gene regulatory networks involved in the differentiation of discrete wing traits. Further, interactions between *apterous* and sex-specific factors such as *double-sex* may have contributed to the origin of sexually dimorphic surface-specific patterns. Finally, we discuss the evolution of eyespot number diversity in the family Nymphalidae within the context of developmental constraints due to *apterous* regulation.

1. Introduction

Butterflies are a group of organisms well known for their diverse and colourful wing patterns. Owing to the dual role these patterns play in survival and mate selection, many butterflies have evolved a signal partitioning strategy where colour patterns appearing on the hidden dorsal surfaces tend to be bright and prominent, generally functioning in sexual signalling, whereas patterns on the exposed ventral surfaces tend to be cryptically coloured and most commonly serve to ward off predators [1,2] (figure 1*a*). The molecular and developmental basis of individual pattern element differentiation, such as eyespots or transverse bands, has been extensively studied [3,4]. Furthermore, we have a functional understanding of the genes involved in differentiating hindwing patterns from forewing patterns [5,6]. However, the molecular mechanisms that lead to striking variations in the development of dorsal versus ventral surface-specific colour patterns remain unknown. Elucidating this process will help us understand the mechanism of diversification and specialization of wing patterns within the butterfly lineage.

A charismatic colour pattern that is present on both dorsal and ventral wing surfaces of a family of butterflies, the nymphalids, is the eyespot. Studies on eyespot evolution through broad comparative work across 400 genera of nymphalid butterflies indicated that eyespots originated around 90 million years ago (MYA) within this family, initially restricted to the ventral hindwing surface [7,8]. The appearance of eyespots on the dorsal surfaces occurred nearly approximately 40 million years (MY) later following redeployment of eyespot gene networks from the ventral surface [8,9]. This surface-specific asymmetry in the evolution of eyespot patterns is intriguing because the molecular mechanisms leading to such evolutionary patterns are unknown and the asymmetry suggests the presence of developmental constraints that might have limited eyespot origins to ventral surfaces only.

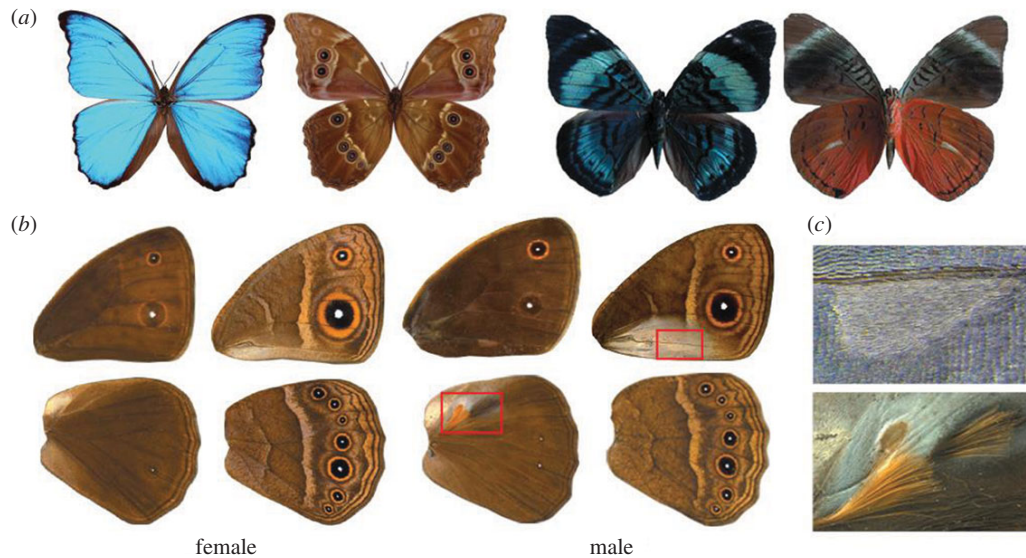


Figure 1. Dorsal-ventral surface-specific variation in butterflies. (a) Dorsal (left) and ventral (right) surfaces of *Morpho menelaus* and *Panacea regina* illustrating striking variation in colour and patterns between surfaces. (b) Dorsal (left) and ventral (right) surfaces of a male and female *Bicyclus anynana*. The regions boxed in red are expanded in c. (c) Magnified view of the androconial organs present only in males. Top: forewing ventral androconia with a characteristic teardrop shape surrounded by silver scales. The scales on the corresponding dorsal forewing surface are completely brown. Bottom: hindwing dorsal androconia, also surrounded by silver scales, along with two patches of hair-pencils. These traits are absent from the ventral hindwing. (Online version in colour.)

We hypothesized that the transcription factor *apterous* (*ap*), a gene expressed on the dorsal wing surfaces of flies [10], might be implicated in differentiating dorsal from ventral wing patterns in butterflies and in constraining the evolution of novel patterns, such as eyespots, asymmetrically across these surfaces. In insects, however, this gene is often present in two copies, *apA* and *apB*, that do not necessarily share the same expression patterns, and flies are unusual for having lost one of these copies. In the beetle *Tribolium castaneum*, *apA* is expressed on the dorsal surface, whereas *apB* is expressed on both surfaces [11]. In the butterfly *Junonia coenia*, *apA* is expressed on the dorsal surface of larval wings [12], but the expression of *apB* and the role of either *apA* or *apB* in wing development and patterning is not known for this or any butterfly species. Here, we study the functions of both copies of *ap* during wing development in the African squinting bush brown *Bicyclus anynana*, which shows dorsal-ventral differences in wing patterns, including a different number of eyespots on these surfaces (figure 1*b,c*). To infer patterns of gene expression of both *ap* copies, we used *in situ* hybridization to localize mRNA expression during wing development. We then used targeted gene knockout using CRISPR/Cas9 to functionally verify the roles of *apA* and *apB* in surface-specific wing patterning and development.

2. Material and methods

(a) Animals

Bicyclus anynana butterflies were reared in a temperature-controlled room at 27°C with a 12:12 h light:dark cycle and 65% humidity. The larvae were fed on corn plants, while the adults were fed on banana.

(b) Cloning and probe synthesis

The *apA* sequence was obtained from [13] and the *apB* sequence was identified from the *B. anynana* genome [14]. The sequences

were amplified with primers specified in electronic supplementary material, table S1, sequenced and then cloned into a PGEM-T Easy vector (Promega). Sense and antisense digoxigenin-labelled (DIG) riboprobes were synthesized *in vitro* using T7 and SP6 polymerases (Roche), purified by ethanol precipitation and resuspended in a 1:1 volume of diethyl pyrocarbonate (DEPC)-treated water:formamide.

(c) *In situ* hybridization

The protocol was modified slightly from [15]. Briefly, larval (last instar caterpillar) or pupal (24–28 h after pupation) wings were dissected in PBS and transferred to glass well plates containing PBST (PBS + 0.1% Tween20) at room temperature. The PBST was then immediately removed and the tissues fixed in 5% formaldehyde for 45 (larval) or 60 min (pupal) on ice, followed by five washes with cold PBST. The tissues were then incubated with 25 $\mu\text{g ml}^{-1}$ proteinase K in cold PBST for 4 (larval) or 5 min (pupal), washed twice with 2 mg ml^{-1} glycine in cold PBST, followed by five washes with cold PBST. For larval wings, the peripodial membrane was then removed on ice, post-fixed for 20 min with 5% formaldehyde and washed with PBST. The wings were gradually transferred to a prehybridization buffer (5X saline sodium citrate (pH 4.5), 50% formamide, 0.1% Tween20 and 100 $\mu\text{g ml}^{-1}$ denatured salmon sperm DNA), washed in the prehybridization buffer and incubated at 60–65°C for 1 h, followed by incubation in hybridization buffer (prehybridization buffer with 1 g l^{-1} glycine and 70 to 140 ng ml^{-1} riboprobe) for 24 h. The wings were then washed 6–10 times in prehybridization buffer at 60–65°C. They were then gradually transferred back to PBST at room temperature, washed five times in PBST and blocked overnight at 4°C (PBST + 1% BSA). The DIG-labelled probes were then detected by incubating the tissues with 1:3000 anti-DIG alkaline phosphatase (Roche) in block buffer for two hours, washed 10 times with block buffer, incubated in alkaline phosphatase buffer (100 mM Tris (pH 9.5), 100 mM NaCl, 5 mM MgCl_2 , 0.1% Tween) and finally stained with NBT/BCIP (Promega) solution at room temperature until colour developed. The reaction was stopped by washing in 2 mM EDTA in PBST and again with

PBST. The samples were either mounted on slides with Immuno-HistoMount medium (Abcam) or post-fixed with 5% formaldehyde before wax embedding and sectioning (Advanced Molecular Pathology Lab, IMCB, Singapore).

(d) Preparation of Cas9 mRNA and guide RNA

pT3TS-nCas9n was a gift from Wenbiao Chen (Addgene plasmid #46757). The plasmid was linearized with XbaI digestion and purified using a GeneJET PCR Purification Kit (Thermo Scientific). Cas9 mRNA was obtained by *in vitro* transcription using the mMESAGE mMACHINE T3 kit (Ambion), tailed using the Poly(A) Tailing Kit (Ambion) and purified by lithium chloride precipitation. The guide RNA templates were prepared using a PCR-based method according to [16]. The candidate targets were manually designed by searching for a GGN₁₈NGG sequence on the sense or antisense strand of *apA* and *apB*, preferably targeting the LIM and homeobox domains of the transcription factor (electronic supplementary material, table S1). They were blasted against the *B. anynana* genome on LepBase.org to check for off-target effects. The template DNA sequence was used to perform an *in vitro* transcription using T7 RNA polymerase (Roche) at 37°C overnight, purified by ethanol precipitation and resuspended in DEPC-treated water.

(e) Microinjections

Eggs were collected on corn leaves within one to two hours of egg laying and were arranged on thin strips of double-sided tape on a Petri dish. Cas9 mRNA and guide RNAs were mixed along with green food dye (electronic supplementary material, table S2) and injected into the eggs with a Borosil glass capillary (World Precision Instruments, 1B100F-3) using a Picospritzer II (Parker Hannifin). A piece of wet cotton was placed in the Petri dish and the eggs were allowed to develop in an incubator at 27°C and high (approx. 80%) humidity. Hatched caterpillars were placed on young corn plants using a brush. Adults that emerged were scored for their phenotypes (electronic supplementary material, table S2). A later set of injections (electronic supplementary material, table S3) was performed to test whether the three sets of guides used (together with Cas9 mRNA) impacted hatching rates relative to injections with Cas9 mRNA alone.

(f) Sequencing and genotyping mutants

Genomic DNA was extracted from leg tissues of mutant individuals using the E.Z.N.A Tissue DNA Kit (Omega Bio-tek). The region surrounding the target sequence was amplified by PCR, purified by ethanol precipitation and used to check for the presence of mutations using the T7 endonuclease I (T7EI) assay. Sequences from individuals with disruptions at the targeted regions were cloned into a PGEM-T Easy vector (Promega) and sequenced.

3. Results

(a) *apA* and *apB* are both expressed on dorsal surfaces of developing wings

We cloned both *ap* homologues from *B. anynana* and used *in situ* hybridization to localize *apA* and *apB* mRNA in developing larval and pupal wing discs. Both homologues of *ap* were localized to the dorsal surfaces of the wings (figure 2*d*; electronic supplementary material, figure S1*b*). In the last larval instar wing discs, *apA* was expressed uniformly on the wing surface but absent in future dorsal eyespot centres of

hindwings (figure 2*a*) and forewings (figure 2*b*). In larval wing discs of the *B. anynana* ‘Spotty’ mutant, which develops two additional dorsal eyespots, *apA* was absent in the additional centres (figure 2*b*). Furthermore, pupal wing expression of both *apA* and *apB* was upregulated in dorsal male-specific cells that give rise to long and thin modified scales, the hair-pencils, used for dispersing pheromones during courtship (figure 2*c*; electronic supplementary material, figure S1*c*). This pattern of expression was not seen in developing female pupal wings, which lack hair-pencils (figure 2*c*; electronic supplementary material, figure S1*c*). Control sense probes for both *apA* and *apB* (electronic supplementary material, figure S1) did not show any surface-specific or hair-pencil-specific staining patterns.

(b) *apA* regulates dorsal surface-specific wing patterning

To functionally test the role of *ap*, we used the CRISPR/Cas9 system to disrupt the homeodomain and LIM domain of *apA* (figure 3*a*) and the LIM domain of *apB* (electronic supplementary material, figure S2*a* and table S2). A range of mosaic phenotypes were observed in both types of *apA* mutant individuals (figure 3; electronic supplementary material, figures S3 and S4). A few of these lacked wings, whose absence was visible upon pupation (electronic supplementary material, figure S3: mutant from batch#9, individual #1(M9-1)), and some adults had mosaic patches of ventral-like scales appearing on the dorsal surface (figure 3*b*: M9-2). In other mutants, the sex pheromone-producing organ, the androconial organ, of the ventral forewing appeared on the dorsal surface in males with its associated silver scales (figure 3*b*: M9-27). Males also had modified hair-pencils associated with the dorsal androconial organ of the hindwing, with loss of characteristic ultrastructure and colouration, and the absence of surrounding silver scales (figure 3*b*: M9-12 (bottom)). Extreme mutant individuals showed improper wing hinge formation, entire wing dorsal to ventral transformation (figure 3*b*: M9-3), the appearance of the ventral white band on the dorsal surface (figure 3*b*: M9-12 (top)), and in one case, all seven eyespots on the dorsal hindwing (figure 3*b*: M9-12 (bottom)), a surface that normally exhibits, on average, zero to one eyespot in males and one to two eyespots in females. *apA* clones also led to an enlarged outer perimeter of the gold ring in dorsal hindwing eyespots (figure 3*b*: M235-11). CRISPR/Cas9 disruption effects on the target sequence were verified in a few individuals, which showed the presence of deletions in the targeted regions (figure 3*a*).

No striking transformations of dorsal to ventral identity were observed in *apB* mutants (electronic supplementary material, figures S2 and S5). Some of the *apB* knockout phenotypes included a wing hinge defect, a missing hindwing in one case (electronic supplementary material, figure S5: B-M9-22) and disturbed margin development (electronic supplementary material, figure S2: B-M9-17), sometimes associated with wing pattern disturbances (electronic supplementary material, figure S2: B-M9-15). Sequencing showed the presence of mutations in the targeted region (electronic supplementary material, figure S2*a*). Injections of the three guides used (*apA* homeodomain, *apA* LIM domain, and *apB* LIM domain) did not significantly alter hatching rates (electronic supplementary material, table S3).

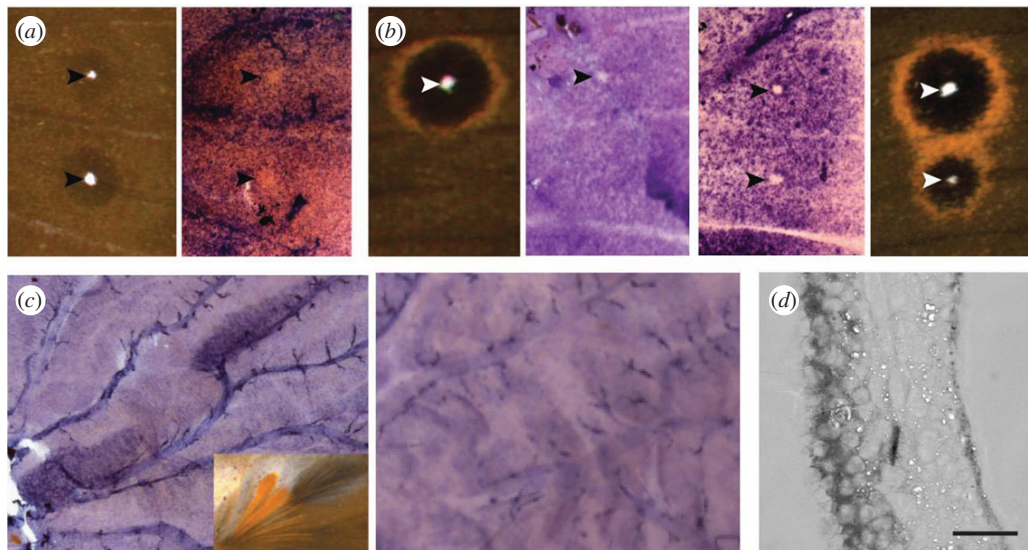


Figure 2. *apA* mRNA localization in developing wing discs of *Bicyclus anynana*. (a) *apA* expression is uniform across the epidermis but absent in future dorsal eyespot centres of hindwings ($n = 5$). (b) *apA* expression is absent in the future dorsal eyespot centre of the wild-type forewing (left) ($n = 3$) and also in the additional eyespot centre in the *B. anynana* 'Spotty' mutant (right) ($n = 7$). (c) Male wings (left) (28 h after pupation) showing upregulated dorsal *apA* expression in the hair-pencil regions. Inset shows the hair-pencils in adult male *B. anynana*. Female wings (right) (25 h after pupation) show no upregulation of *apA* in corresponding regions of the dorsal surface. (d) Cross-sectional view of a developing wing disc showing dorsal-specific *apA* expression (left side of the cross section). Scale bar, 20 μm . (Online version in colour.)

Knockdown of *apA* in a variety of insects from different lineages indicates that *apA* is necessary for wing growth and development and its function in this process seems to be highly conserved [10,11,17]. However, our experiments, in agreement with others, also indicate a varying degree of co-option of this transcription factor or one of its downstream effectors into late wing development processes such as wing patterning and exoskeletalization. In *T. castaneum*, RNAi knockdown of *apA* and *apB* individually shows almost no phenotypic effects, while their simultaneous knockdown leads to more dramatic phenotypes such as elytral exoskeletalization defects, depending on the developmental stage. Therefore, both *apA* and *apB* in beetles are important for early and late wing developmental processes [11]. In *B. anynana*, knockout of both *apA* and *apB* causes defects in early wing development, but only *apA* or one of its downstream targets appears to have been co-opted to control dorsal surface-specific wing patterning.

(c) *apA* functions both as an activator and repressor of wing traits

Interestingly, our work shows that *apA* has multiple different, often antagonistic functions in surface- and sex-specific development between the fore- and hindwings. For example, *apA* acts as a repressor of male androconial organs and silver scale development on dorsal forewings, while it promotes hair-pencil and silver scale development on the dorsal hindwings of males (figure 4a). These effects point to the likely interaction between *apA* and other factors such as sex-specific (*doublesex*) or wing-specific (*Ultrabithorax*) factors that together can specify sex- and wing-specific pattern development. We previously showed that *Ultrabithorax* (*Ubx*) is expressed in the hindwings but not forewings of *B. anynana* [20]. In addition, the presence of a gene from the sex determination pathway, *doublesex* (*dsx*), in the future androconial regions of male wings of *B. anynana* was also verified by *in situ* hybridization

and semi-quantitative PCR [21]. These data support a likely combinatorial function reminiscent of the interactions between the hox gene *Scr* and *dsx* in the determination of the male-specific sex combs in the legs of *D. melanogaster* [22]. The presence or absence of *Ubx*, type of *dsx* splice variant, and *apA* may be sufficient to give each sex and wing surface a unique identity, though more work needs to be done to test this hypothesis. Given that proteins of the LIM-homeodomain subfamily, to which *ap* belongs, are unique in their ability to bind other proteins via their LIM domain [23], their involvement in such a large range of developmental processes, as repressors and activators, is likely.

4. Discussion and conclusion

Mutations in *apA* point to this gene functioning as a dorsal surface selector in *B. anynana* butterflies. Selector genes comprise a small set of developmental genes that are critical for specifying cell, tissue, segment or organ identities in organisms [24]. The wing selector hox gene *Ubx* allows hindwings to have a different identity from forewings. For example, the restricted expression of *Ubx* in hindwings of most insects examined so far is required for membranous wing formation in beetles and bugs [25], haltere formation in flies [26] and hindwing-specific colour patterns in butterflies [6]. When *Ubx* is mutated, in all the examples described above, hindwings acquire the identity of forewings, and when *Ubx* is overexpressed in forewings, these acquire a more hindwing-like identity [20]. In *B. anynana*, *apA* functions in a similar manner along the dorsal–ventral axis of each wing—mutations in this gene make dorsal wing surfaces acquire a ventral identity. This type of homeotic mutation was also observed in a limited way, in bristles along the margin of the wings of *D. melanogaster*, where *ap* mutant clones developed bristles with a ventral identity [27]. *Bicyclus anynana*, however, appears to have made inordinate use of *apA* for surface-specific colour patterning and sexual trait

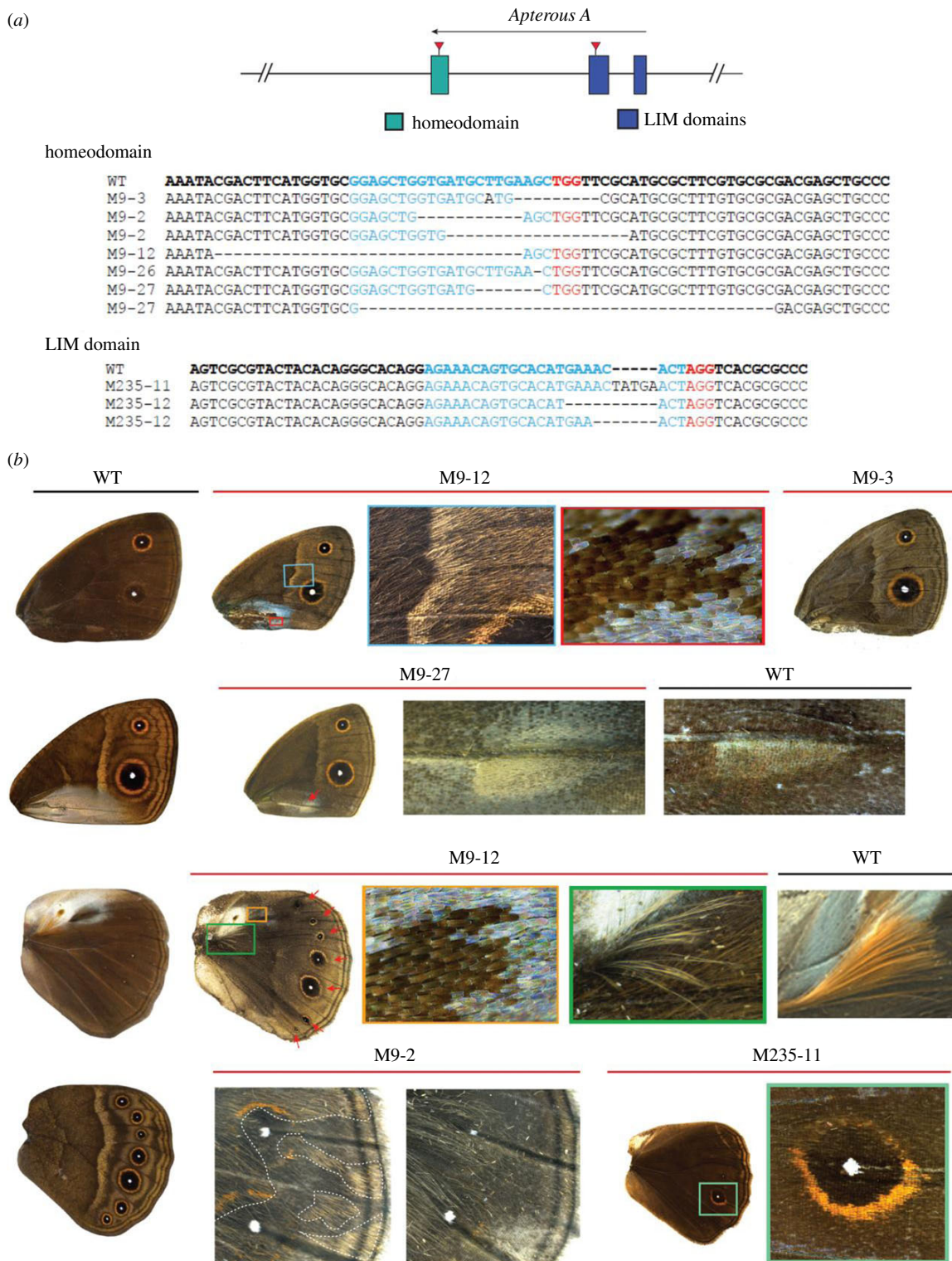


Figure 3. CRISPR/Cas9 mosaic wing pattern phenotypes of *apA* knockouts. (a) Top: regions of the *apA* gene in *B. anynana* targeted using the CRISPR/Cas9 system. Bottom: sequences of the homeodomain and LIM domain regions of mutant individuals compared with the wild-type sequence in bold. Blue is the region targeted and the PAM sequence is in red. Deletions are indicated with '-'. (b) A subset of the CRISPR/Cas9 *apA* mutant phenotypes observed in *B. anynana*. The left column shows the wild-type (WT) dorsal and ventral surfaces for male forewings and hindwings. M9-12 (top): the dorsal forewing of a mutant male highlighting some of the ventral-like phenotypes and defects. The boxed regions are expanded to show the appearance of ventral-like white band and silver scales. M9-3: dorsal forewing surface of a mutant female resembling the ventral surface. M9-27: mutant with the ventral teardrop shape forewing androconial organ appearing on the dorsal surface (red arrow). WT dorsal forewing androconia is shown for comparison. M9-12 (bottom): a mutant dorsal hindwing with the appearance of all seven eyespots (red arrows), normally only seen on the ventral surface. The boxed regions are expanded to show the loss of silver scales associated with the dorsal hindwing androconia and improper development of hair-pencils. WT hair-pencil is shown for comparison. M9-2: mosaic phenotype (left) on the dorsal surface with ventral-like light coloured scales. Clones are indicated with a dashed white line. Corresponding region of the other wing of the same individual (right) shows no mosaicism. M235-11: a dorsal hindwing of a mutant with the width of the gold ring resembling that of ventral eyespots. (Online version in colour.)

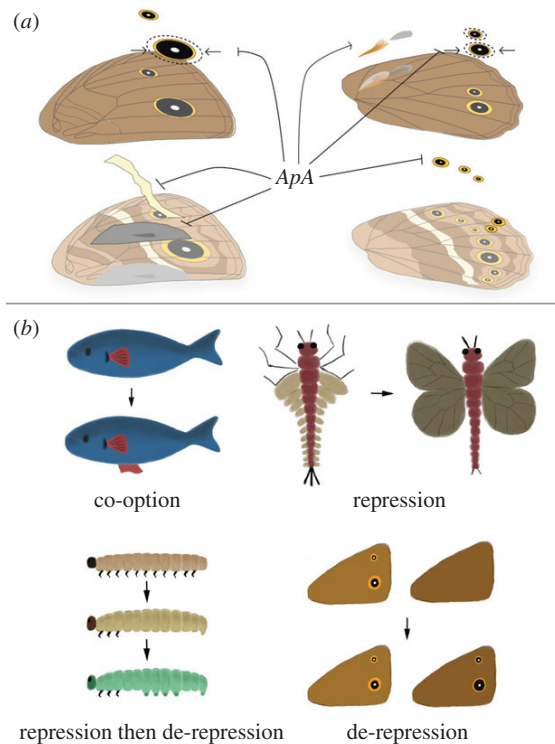


Figure 4. The role of *apterous* in surface-specific wing patterning in *B. anynana* and evolution of serial homologues in butterflies. (a) A schematic of the different functions of *apA* on the dorsal surface of *B. anynana*. *apA* acts as a repressor of ventral traits such as the white transversal band, forewing androconia, hindwing eyespots and the outer perimeter of the gold ring, and acts as an activator of hindwing hair-pencils and silver scales. (b) Different modes of serial homologue evolution involving the co-option of a (fin) gene network to a novel body location [18], repression of the ancestrally repeated (wing) network in a subset of body segments (adapted from [19]), repression followed by de-repression of the (limb) network in certain body segments [5] and de-repression of a never-expressed (eyespot) network at a novel body location. (Online version in colour.)

development across the entire wing, which is a novel described role for this gene across insects.

Further, this work highlights the possible role of *apA* in restricting the origin and early evolution of serial homologues such as eyespots in nymphalid butterflies to the ventral surface of the wings only. The appearance of additional eyespots on the dorsal surface of hindwings in *apA* mutants, and the absence of *apA* mRNA at the precise position where a few dorsal eyespots develop in both fore- and hindwings at the stage of eyespot centre differentiation, implicates *apA* as a repressor of eyespot development. The additional gaps in *apA* expression observed in Spotty mutants further suggests that genetic mechanisms of eyespot number evolution on the dorsal surface proceeded via local repression of *apA*. We propose, thus, that the original ventral restriction of eyespots was due to the ancestral presence of *apA* on dorsal wing surfaces, and that eyespots' later appearance on these surfaces was due to local *apA* repression.

References

- Kemp DJ. 2007 Female butterflies prefer males bearing bright iridescent ornamentation. *Proc. R. Soc. B* **274**, 1043–1047. (doi:10.1098/rspb.2006.0043)
- Prudic KL, Stoehr AM, Wasik BR, Monteiro A. 2015 Eyespots deflect predator attack increasing fitness

The ancestral presence of a repressor (*apA*) of a gene regulatory network in a specific body location, followed by repression of the repressor, seems to represent a novel mode of serial homologue diversification (figure 4b). This mode of serial homologue diversification is similar but also distinct from the mechanism previously proposed to lead to the reappearance of abdominal appendages in lepidopteran larvae—via local repression of the limb repressor *hox* protein, *Abdominal-A* (*Abd-A*) [5,28]. In contrast to eyespots, when arthropod appendages first originated, they were probably present in every segment of the body [29]. Limbs were later repressed in abdominal segments, and finally they were de-repressed in some of these segments in some insect lineages [5]. So, while the last steps of abdominal appendage and eyespot number diversification are similar (de-repression of a repressed limb/eyespot network), the early stages are different.

Comparative work across nymphalid butterflies also showed that the origin of dorsal eyespots was dependent on the presence of corresponding ventral eyespots in ancestral lineages [9]. This implies that the extant diversity of eyespot patterns is biased/limited due to developmental constraints, probably imposed by *apA*. Interestingly, while approximately 99% of the species in our database display such constraints, i.e., dorsal eyespots always having ventral counterparts, a few butterflies (such as *Argyrophenax anti-podium* or *Cassionympha cassius*) display dorsal eyespots that lack ventral counterparts. The molecular basis for these rare patterns remains to be explored.

In summary, we uncovered a key transcription factor, *apA*, that due to its restricted expression on dorsal wing surfaces allowed *B. anynana* butterflies to develop and evolve their strikingly different dorsal and ventral wing patterns under natural and sexual selection. The interaction of *apA* with other sex- and wing-specific factors may explain the surface-specific pattern diversity we see across this as well as other butterfly species, but future comparative work is needed to further test these hypotheses. Additionally, our work has identified a new system to examine how developmental constraints, via *apA* repression of eyespot development, have shaped eyespot number biodiversity.

Ethics. No animal experimentation permits were required for the experiments conducted here. *Bicyclus anynana* butterflies have been reared in the laboratory since 1988 and were imported under an AVA permit to the laboratory in Singapore.

Data accessibility. All data supporting this article are provided in the main text or as part of the electronic supplementary material.

Authors' contributions. A.P. and A.M. designed the study. A.P. performed the research and analysed the data. A.P. and A.M. wrote the manuscript. All the authors gave their final approval for publication.

Competing interests. We declare we have no competing interests.

Funding. This work was funded by Ministry of Education, Singapore grant R-154-000-602-112, the National University of Singapore grant R-154-000-587-133 and by the Department of Biological Sciences, NUS.

Acknowledgements. We thank Arjen van't Hof and Luqman Aslam for their help in retrieving sequence information from the *B. anynana* genome, Mainak Das Gupta for his help in the *in situ* hybridization protocols and Monteiro lab members for their support.

- and promoting the evolution of phenotypic plasticity. *Proc. R. Soc. B* **282**, 20141531. (doi:10.1098/rspb.2014.1531)
3. Monteiro A. 2015 Origin, development, and evolution of butterfly eyespots. *Annu. Rev. Entomol.* **60**, 253–271. (doi:10.1146/annurev-ento-010814-020942)
 4. Martin A, Reed RD. 2010 Wingless and aristaless2 define a developmental ground plan for moth and butterfly wing pattern evolution. *Mol. Biol. Evol.* **27**, 2864–2878. (doi:10.1093/molbev/msq173)
 5. Warren R, Nagy L, Selegue J, Gates J, Carroll S. 1994 Evolution of homeotic gene regulation and function in flies and butterflies. *Nature* **372**, 458–461. (doi:10.1038/372458a0)
 6. Weatherbee SD, Nijhout HF, Grunert LW, Halder G, Galant R, Selegue J, Carroll S. 1999 Ultrabithorax function in butterfly wings and the evolution of insect wing patterns. *Curr. Biol.* **9**, 109–115. (doi:10.1016/S0960-9822(99)80064-5)
 7. Oliver JC, Tong X, Gall LF, Piel WH. 2012 A single origin for Nymphalid butterfly eyespots followed by widespread loss of associated gene expression. *PLoS Genet.* **8**, e1002893. (doi:10.1371/journal.pgen.1002893)
 8. Oliver JC, Beaulieu JM, Gall LF, Piel WH, Monteiro A. 2014 Nymphalid eyespot serial homologues originate as a few individualized modules. *Proc. R. Soc. B* **281**, 20133262. (doi:10.1098/rspb.2013.3262)
 9. Schachat SR, Oliver JC, Monteiro A. 2015 Nymphalid eyespots are co-opted to novel wing locations following a similar pattern in independent lineages. *BMC Evol. Biol.* **15**, 20. (doi:10.1186/s12862-015-0300-x)
 10. Cohen B, McGuffin ME, Pfeifle C, Segal D, Cohen SM. 1992 Apterous, a gene required for imaginal disc development in *Drosophila* encodes a member of the LIM family of developmental regulatory proteins. *Genes Dev.* **6**, 715–729. (doi:10.1101/gad.6.5.715)
 11. Tomoyasu Y, Arakane Y, Kramer KJ, Denell RE. 2009 Repeated co-options of exoskeleton formation during wing-to-elytron evolution in beetles. *Curr. Biol.* **19**, 2057–2065. (doi:10.1016/j.cub.2009.11.014)
 12. Carroll SB, Gates J, Keys DN, Paddock SW, Panganiban GE, Selegue JE, Williams JA. 1994 Pattern formation and eyespot determination in butterfly wings. *Science* **265**, 109–114. (doi:10.1126/science.7912449)
 13. Conceicao IC, Long AD, Gruber JD, Beldade P. 2011 Genomic sequence around butterfly wing development genes: annotation and comparative analysis. *PLoS ONE* **6**, e23778. (doi:10.1371/journal.pone.0023778)
 14. Nowell RW *et al.* 2017 A high-coverage draft genome of the mycalesine butterfly *Bicyclus anynana*. *Gigascience* **6**, 1–7. (doi:10.1093/gigascience/gix035)
 15. Ramos D, Monteiro A. 2007 *In situ* protocol for butterfly pupal wings using riboprobes. *J. Vis. Exp.* **4**, 208. (doi:10.3791/208)
 16. Bassett AR, Tibbit C, Ponting CP, Liu JL. 2013 Highly efficient targeted mutagenesis of *Drosophila* with the CRISPR/Cas9 system. *Cell Rep.* **4**, 220–228. (doi:10.1016/j.celrep.2013.06.020)
 17. Liu FZ, Li KY, Li J, Hu DB, Zhao J, He YP, Zou YL, Feng YN, Hua HX. 2015 *Apterous a* modulates wing size, bristle formation and patterning in *Nilaparvata lugens*. *Sci. Rep.* **5**, 1–12. (doi:10.1038/srep10526)
 18. Ruvinsky I, Gibson-Brown JJ. 2000 Genetic and developmental bases of serial homology in vertebrate limb evolution. *Development* **127**, 5233–5244. (doi:11076746)
 19. Carroll SB, Weatherbee SD, Langeland JA. 1995 Homeotic genes and the regulation and evolution of insect wing number. *Nature* **375**, 58–61. (doi:10.1038/375058a0)
 20. Tong X, Hrycaj S, Podlaha O, Popadic A, Monteiro A. 2014 Over-expression of *Ultrabithorax* alters embryonic body plan and wing patterns in the butterfly *Bicyclus anynana*. *Dev. Biol.* **394**, 357–366. (doi:10.1016/j.ydbio.2014.08.020)
 21. Bhardwaj S, Prudic KL, Bear A, Das Gupta M, Wasik BR, Tong X, Cheong WF, Wenk MR, Monteiro A. 2018 Sex differences in 20-hydroxyecdysone hormone levels control sexual dimorphism in *Bicyclus anynana* butterfly wing patterns. *Mol. Biol. Evol.* **35**(2), 465–472.
 22. Tanaka K, Barmina O, Sanders LE, Arbeitman MN, Kopp A. 2011 Evolution of sex-specific traits through changes in HOX-dependent doublesex expression. *PLoS Biol.* **9**, e1001131. (doi:10.1371/journal.pbio.1001131)
 23. Hobert O, Westphal H. 2000 Functions of LIM-homeobox genes. *Trends Genet.* **16**, 75–83. (doi:10.1016/S0168-9525(99)01883-1)
 24. Mann R, Carroll S. 2002 Molecular mechanisms of selector gene function and evolution. *Curr. Opin. Genet. Dev.* **12**, 592–600. (doi:10.1016/S0959-437X(02)00344-1)
 25. Whitney M, Tomoyasu Y, Wheeler SR, Denell RE. 2005 *Ultrabithorax* is required for membranous wing identity in the beetle *Tribolium castaneum*. *Nature* **433**, 643–647. (doi:10.1038/nature03272)
 26. Lewis EB. 1963 Genes and developmental pathways. *Am. Zool.* **3**, 33–56. (doi:10.1093/icb/3.1.33)
 27. Diaz-Benjumea FJ, Cohen SM. 1993 Interaction between dorsal and ventral cells in the imaginal disc directs wing development in *Drosophila*. *Cell* **75**, 741–752. (doi:10.1016/0092-8674(93)90494-B)
 28. Suzuki Y, Palopoli M. 2001 Evolution of insect abdominal appendages: are prolegs homologous or convergent traits? *Dev. Genes Evol.* **211**, 486–492. (doi:10.1007/s00427-001-0182-3)
 29. Shubin N, Tabin C, Carroll S. 1997 Fossils, genes and the evolution of animal limbs. *Nature* **388**, 639–648. (doi:10.1038/41710)